

CASCADE PID-LQR CONTROL STRATEGY FOR NONLINEAR FLEXIBLE INVERTED PENDULUM SYSTEM

Thi-Hong-Lam Le*, Khanh-Hung Pham, Dinh-Luan Pham, Gia-Dat Tong,
Le-Thanh-Dat Nguyen, Trinh-Anh-Tuan Ngo, Xuan-Tuan Le, Minh-Tuan Nguyen

¹Ho Chi Minh City University of Technology and Education (HCMUTE)
Vo Van Ngan St., No.01, Thu Duc city, Ho Chi Minh City, 700000, Vietnam

* Corresponding author. E-mail: lamlth@hcmute.edu.vn

Abstract: This study presents a simulation-based investigation into the application of a Cascade Proportional-Integral-Derivative (PID) combined with Linear Quadratic Regulator (LQR) control scheme for managing the complexities of a Nonlinear Flexible Inverted Pendulum System (NFIPS). The NFIPS, characterized by nonlinear dynamics and structural flexibility, demands a sophisticated control strategy to achieve stable and precise performance. The proposed Cascade PID-LQR scheme integrates the advantages of PID for addressing nonlinearities and LQR for optimizing linearized dynamics. Through comprehensive simulations, the effectiveness of the proposed control scheme is evaluated, emphasizing its potential in enhancing stability, response speed, and robustness. The study contributes valuable insights into the application of advanced control methodologies in handling nonlinear and flexible systems, paving the way for further exploration and practical implementations in related domains such as robotics and mechatronics.

Keywords: Nonlinear flexible inverted pendulum, NFIPS, cascade PID-LQR controller, stabilization control.

1. Introduction

A nonlinear flexible inverted pendulum system (NFIPS) is a new model in family pendulum, which is an unpopular model in research. NFIPS is a highly nonlinear, unstable system, and hard to control in simulation or reality. NFIPS is built by adding a flexible single link, which is a flexible link with an end weight, to a single inverted pendulum system (SIP).

With SIP, this is a classic inverted pendulum system and is widely used in teaching and researching control theory around the world. SIP consists of a stiff single rod mounted on a linear cart whose axis of rotation is perpendicular to the direction of motion of the cart. Currently, it is effortless to find research on SIP with various algorithms, such as a PID controller [1], [2], [3], [4], [5], a LQR controller [6], [7], a fuzzy controller [8], [9], a neural network controller [10], [11], etc. As for a flexible single inverted pendulum system (FIP), this system is less frequently proposed and researched. Instead of using a stiff link, FIP is built by using a flexible and resilient link with an end weight. Currently, a few research groups investigated and published this system. Such as FIP was researched and approached by applying linear quadratic control using a personal computer [12]. Besides, FIP was also proposed and implemented to apply a robust control approach for flexible inverted pendulum [13]. Another study presented a dynamic model of a planar flexible inverted pendulum system under the frame of multi-body dynamics in a floating frame of reference formulation [14]. In this research, the designed controller with a simple low-pass filter for the flexible inverted pendulum was validated by the simulation of a simple flexible pendulum sample.

Because NFIPS is made up of the characters of SIP and FIP, which are presented above. Therefore, NFIPS is more complex and become a big problem challenges researchers in control theory field. Currently, there is very little research on NFIPS. Consequently, the authors decided to explore this system and apply Cascade PID-LQR control strategy. The main goal of this research is to calculate mathematical modeling system of NFIPS and implement Cascade PID-LQR for NFIPS in simulation with disturbance.

The structure of this paper is organized as follows: Part 1 introduces NFIPS, and relevant papers are published around the world. In Part 2, mathematical modeling of NFIPS is investigated and presented. In Part 3 of the article, Cascade PID-LQR controller is proposed and designed for NFIPS. The simulation results of NFIPS with Cascade PID-LQR controller are presented in Part 4. And finally, the conclusion and development directions of the article are presented in Part 5.

2. Mathematical Modeling of NFIPS

NFIPS is a highly nonlinear, unstable, and flexible system. This system has two main components: the cart operates with a servo motor. Besides, the flexible pendulum is a flexible link with an end weight and the stiff pendulum is the long pendulum.

The mathematical modeling of NFIPS involves describing the dynamic behavior of the system using equations in matrix form (1) – (13). Besides, NFIPS structure is shown in Fig. 1, definitions of dimensions and rotation angles defining pendulum position are also shown in Tab. 1.

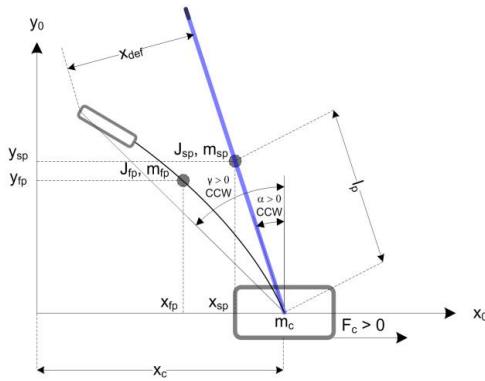


Fig. 1. Flexible pendulum conventions

Tab. 1. The NFIPS structure characteristics and system parameters

System Structure Characteristic	Definition	Value
x_c	Position of cart	na
α	Angle of stiff pendulum	na
γ	Angle of flexible pendulum	na
F_c	An applied force	na
x_{def}	Distance between the tip of stiff pendulum and the tip of flexible pendulum	na
m_c	Mass of cart	0.085 (kg)
m_{sp}	Mass of stiff pendulum	0.15 (kg)
l_{sp}	Distance of the center of mass	0.14 (m)
m_{fp}	Mass of flexible pendulum	0.007 (kg)
l_{fp}	Distance of the center of mass	0.1 (m)
K_s	Stiffness of the flexible pendulum	0.21
g	Gravity	9.81(m/s ²)

According to [15], the dynamical equation is calculated and presented in the form of an equation of state as follows:

$$\begin{bmatrix} H_{11} & H_{12} & H_{13} \\ H_{21} & H_{22} & H_{23} \\ H_{31} & H_{32} & H_{33} \end{bmatrix} \begin{bmatrix} \ddot{x}_c \\ \ddot{\alpha} \\ \ddot{\gamma} \end{bmatrix} + \begin{bmatrix} M_1 \\ M_2 \\ M_3 \end{bmatrix} = \begin{bmatrix} F_c \\ 0 \\ 0 \end{bmatrix} \quad (1)$$

where

$$H_{11} = (m_{fp} + m_c + m_{sp}) \quad (2)$$

$$H_{12} = (-m_{sp}l_{sp} \cos(\alpha) - m_{fp}l_{sp} \cos(\alpha)) \quad (3)$$

$$H_{13} = 0 \quad (4)$$

$$H_{21} = -m_{sp}l_{sp} \cos(\alpha) - m_{fp}l_{sp} \cos(\alpha) \quad (5)$$

$$H_{22} = J_{sp} + m_{fp}l_{fp}^2 + m_{sp}l_{sp}^2 \quad (6)$$

$$H_{23} = m_{fp}l_{fp} \sin(\gamma)l_{sp} \sin(\alpha) + m_{fp}l_{fp} \cos(\gamma)l_{sp} \cos(\alpha) \quad (7)$$

$$H_{31} = -m_{fp}l_{fp} \cos(\gamma) \quad (8)$$

$$H_{32} = m_{fp}l_{fp} \sin(\gamma)l_{sp} \sin(\alpha) + m_{fp}l_{fp} \cos(\gamma)l_{sp} \cos(\alpha) \quad (9)$$

$$M_1 = (m_{sp}l_{sp} \sin(\alpha) + m_{fp}l_{fp} \sin(\alpha))\dot{\alpha}^2 + m_{fp}l_{fp} \sin(\gamma)\dot{\gamma}^2 - m_{fp}l_{fp} \cos(\gamma)\dot{\gamma} \quad (10)$$

$$M_2 = [-m_{fp}l_{fp} \sin(\gamma)l_{sp} \cos(\alpha) + m_{fp}l_{fp} \cos(\gamma)l_{sp} \sin(\alpha)]\dot{\gamma}^2 - m_{sp}gl_{sp} \sin(\alpha) - m_{fp}gl_{fp} \sin(\alpha) \quad (11)$$

$$M_3 = [-m_{fp}l_{fp} \cos(\gamma)l_{sp} \sin(\alpha) + m_{fp}l_{fp} \sin(\gamma)l_{sp} \cos(\alpha)]\dot{\alpha}^2 - m_{fp}gl_{fp} \sin(\gamma) + K_s\gamma \quad (12)$$

Referring to [15], the force applied to the cart of NFIPS, which is produced by the servo motor and can be expressed by the following equation.

$$F_c = \frac{\eta_g K_g K_t}{R_m r_{mp}} \left(-\frac{K_g K_m \dot{x}_c}{r_{mp}} + \eta_m V_m \right) \quad (13)$$

Therefore, the state equation (1) and equation (13) present the dynamic equations of NFIPS. The parameters of the servo motor are listed in

Tab. 2.

Tab. 2. Parameters of servo motor

Symbol	Description	Value
η_g	Planetary gearbox efficiency	0.9
K_g	Planetary gearbox gear ratio	3.71
K_t	Motor current-torque constant	7.68*10 ⁻³ (N m/A)
K_m	Motor back-emf constant	7.68*10 ⁻³ (V/(rad/s))
r_{mp}	Motor pinion radius	6.35*10 ⁻³ (m)
η_m	Motor efficiency	0.69
R_m	Motor armature resistance	2.6 (Ω)

After calculating the dynamic equation of NFIPS, we implement this system to linearize. For NFIPS, the state of the system is defined by:

$$x = [x_c \quad \dot{x}_c \quad \alpha \quad \dot{\alpha} \quad \gamma \quad \dot{\gamma}]^T \quad (14)$$

And the dynamic equation of NFIPS is linearized about the zero-angle position.

$$\begin{aligned} x_c = 0; \dot{x}_c = 0; \alpha = 0; \\ \dot{\alpha} = 0; \gamma = 0; \dot{\gamma} = 0 \end{aligned} \quad (15)$$

The linearized state equations of NFIPS are shown below:

$$\begin{cases} \dot{x} = Ax + Bu \\ y = Cx \end{cases} \quad (16)$$

Matrices A and B are calculated by equations (17) and (18). The values of them are presented in Appendix A of this paper.

$$A = \begin{bmatrix} 0 & 1 & 0 & 0 & 0 & 0 \\ \frac{\partial(\ddot{x}_c)}{\partial \dot{x}_c} & \dots & \dots & \dots & \dots & \frac{\partial(\ddot{x}_c)}{\partial \lambda} \\ 0 & 0 & 1 & 0 & 0 & 0 \\ \frac{\partial(\ddot{\alpha})}{\partial \dot{x}_c} & \dots & \dots & \dots & \dots & \frac{\partial(\ddot{\alpha})}{\partial \dot{x}_c} \\ 0 & 0 & 0 & 0 & 1 & 0 \\ \frac{\partial(\ddot{\lambda})}{\partial \dot{x}_c} & \dots & \dots & \dots & \dots & \frac{\partial(\ddot{\lambda})}{\partial \dot{x}_c} \end{bmatrix} \quad (17)$$

$$B = \begin{bmatrix} 0 & \frac{\partial(\ddot{x}_c)}{V_m} & 0 & \frac{\partial(\ddot{\alpha})}{V_m} & 0 & \frac{\partial(\ddot{\gamma})}{V_m} \end{bmatrix}^T \quad (18)$$

Subsequently, the controllability of NFIPS is discussed. T matrix is established to examine the controllability of this system. The T matrix is as follows:

$$T = [B \ AB \ A^2B \ A^3B \ A^4B \ A^5B] \quad (19)$$

From Tab. 1,

Tab. 2, equations (17), (18). The rank and $\det(T)$ of NFIPS are calculated as follows:

$$\text{rank}(T) = 6; \det(T) = -8.0272e + 14 \quad (20)$$

Because $\det(T)$ does not equal zero and the matrix's rank is equal to the number of systematic degrees. This makes the system controllable.

3. Cascade PID-LQR controller

NFIPS is a nonlinear dynamic with structural flexibility. Consequently, a combined controller is proposed, and this is a Cascade PID-LQR controller, which is designed by combining PID algorithm and LQR algorithm. PID algorithm is a popular and widely used in various control system. Form of the PID controller is given by

$$G_C(s) = K_p + \frac{K_I}{s} + K_D s \quad (21)$$

In addition, LQR algorithm is also appreciated and commonly used in controlling balance in many systems. The control law of LQR controller is given as:

$$u(t) = -Kx(t) \quad (22)$$

The Cascade PID-LQR controller scheme for NFIPS is presented as follows:

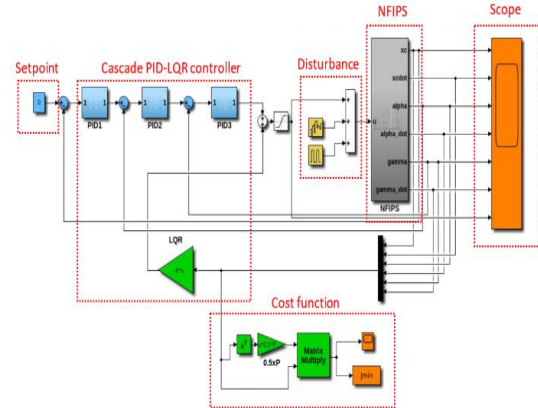


Fig. 2. Simulink model for NFIPS with Cascade PID-LQR controller

The selected parameters for the PID controller are as follows:

$$\begin{aligned} K_{P_1} = 2; K_{I_1} = 0.5; K_{D_1} = 0.1 \\ K_{P_2} = 1; K_{I_2} = 0.08; K_{D_2} = 0.02 \\ K_{P_3} = 1; K_{I_3} = 0.01; K_{D_3} = 0.05 \end{aligned} \quad (23)$$

Q, R matrices of LQR controller are chosen as follows:

$$\begin{aligned} Q = \text{diag}\{10^4, 0.1, 10^3, 0.1, 10^3, 0.1\} \\ R = 1 \end{aligned} \quad (24)$$

K control matrix is calculated by $lqr(A,B,Q,R)$ command in MATLAB. The resulting matrix is shown below as follows:

$$K(1 \times 6) = [-100.0000 \ -62.0681 \ 151.6449 \ 33.5191 \ 20.7312 \ -1.3042] \quad (25)$$

4. Validation

4.1. Stability under Varying Disturbance Magnitudes

The key point of this subsection is to evaluate the controller's performance under varying disturbance magnitudes.

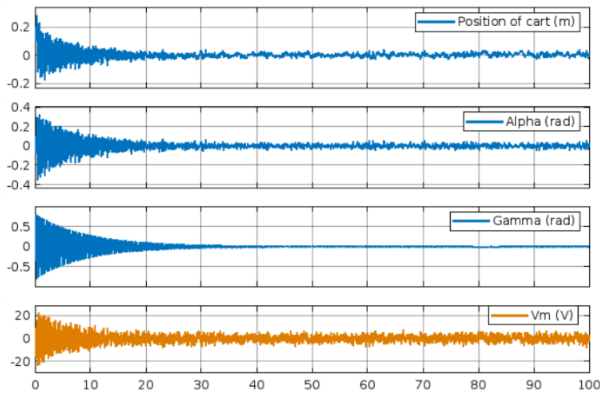


Fig. 3. The response of NFIPS under disturbance input

The results show that the Cascade PID-LQR controller can effectively control NFIPS under a disturbance input. It takes NFIPS approximately 40 seconds to be stabilized. The position of cart, the angle of the stiff pendulum, and the angle of the flexible pendulum can both remain balanced in zero-angle position. In addition, input disturbances affected the control quality, with the position of the cart and the angle of the stiff pendulum being more affected. The values of two output parameters fluctuate within the range of $[-0.05; 0.05]$ (rad). However, affection for an angle of the flexible pendulum is not significant.

4.2. Closed-Loop Stability and Tracking Performance

Main objective of this subsection is to evaluate the closed-loop stability and tracking performance of the Cascade PID-LQR control scheme for NFIPS under normal operating conditions without disturbances. This test case aims to verify the controller's performance under normal conditions, providing insights into its ability to maintain stability and achieve accurate trajectory tracking without the influence of external disturbances.

The time for NFIPS to stabilize is very similar to the case which is analyzed above. It also takes NFIPS approximately 40 seconds to stabilize. In this case, the values of four output parameters are not appeared to fluctuate from this system which is stabilize.

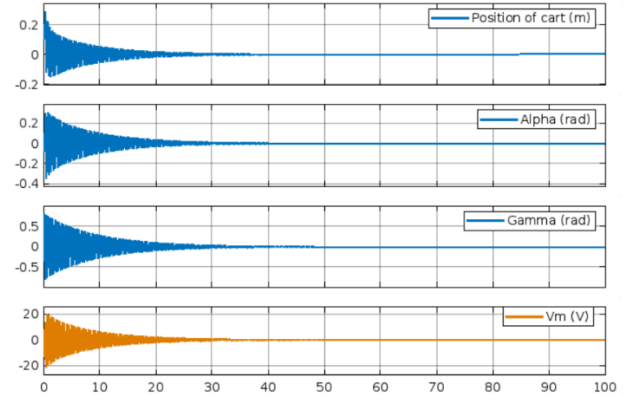


Fig. 4. The response of NFIPS without disturbance

4.3 Disturbance and Pulse Generator Input

Main point of this test case is to evaluate the robustness and performance of the Cascade PID-LQR control scheme for a Nonlinear Flexible Inverted Pendulum System under the influence of disturbance and pulse generator inputs. This test case aims to assess the controller's performance in the presence of disturbances and pulse inputs, providing insights into its robustness and disturbance rejection capabilities.

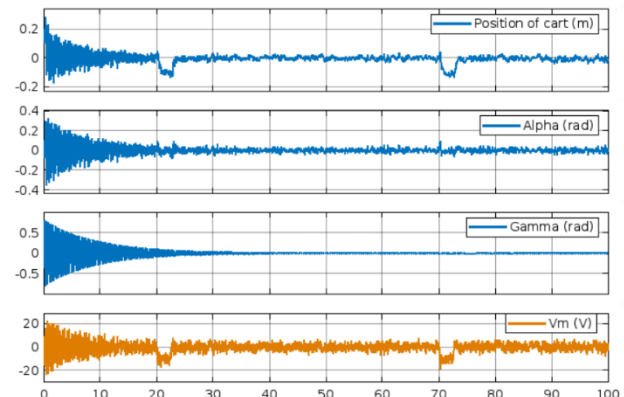


Fig. 5. The response of NFIPS under disturbance and pulse generator inputs

In this case, under disturbance and pulse generator inputs, the response of the NFIPS is greatly affected. Specifically, the error of the cart position is sometimes up to 0.18 (rad) compared to zero. For the angle of the stiff pendulum, the value of it fluctuates within the range of $[-0.05; 0.05]$ (rad). In general, the response of the angle of the stiff pendulum is relatively like two cases which are presented above. Likewise, the angle of the flexible pendulum is also not much affected by disturbance and pulse generator inputs.

In all three cases which are presented above, the cost function of this system consistently approaches zero. This shows that the cascade PID-LQR controller has good control the system and helps cost function always reach the value 0.

5. Conclusions

In conclusion, the study on the application of the Cascade PID combined with LQR control scheme for the NFIPS in simulation has yielded valuable insights into the system's control performance. The integration of Cascade PID and LQR controllers has shown promising results in achieving stability and effective trajectory tracking for the NFIPS.

Through the simulation experiments, the authors observed that the Cascade PID-LQR control scheme effectively mitigated the challenges posed by the nonlinear and flexible nature of the inverted pendulum system. The combination of PID control with the LQR further enhanced the system's overall control performance.

The controller demonstrated its capability to stabilize the NFIPS and accurately follow predefined reference trajectories. The closed-loop stability was maintained, showcasing the effectiveness of the control strategy in handling inherent nonlinearities and uncertainties present in the system.

While the study was limited to simulation environments, the positive outcomes suggest the potential applicability of the Cascade PID-LQR control scheme to real-world scenarios with a NFIPS. Future work may involve experimental validations and parameter tuning to further refine the controller for practical implementation. Overall, the study contributes to the understanding and development of advanced control strategies for challenging dynamic systems.

6. Appendix A

The values of matrices A and B are as follows:

$$A = \begin{bmatrix} 0 & 1 & 0 & 0 & 0 & 0 \\ 0 & -35.1281 & 2.1568 & 0 & 0.2542 & 0.0035 \\ 0 & 0 & 0 & 1 & 0 & 0 \\ 0 & -69.6836 & 23.7460 & 0 & 2.7993 & 0.0070 \\ 0 & 0 & 0 & 0 & 0 & 1 \\ 0 & -2.2008 & -0.1013 & 0 & -259.3841 & 0.0002 \end{bmatrix}$$

$$B = [0; 5.4018; 0; 10.7156; 0; 0.3384]$$

The program of mathematical modeling of NFIPS is given below:

```
clc
clear all
close all
% Flexible inverted pendulum system -
FLEXIP%
% LQT control of FLEXIP %
% Modeling script %
% 1st version on Dec 24 2023 %
```

```
%% system paras %%
% x1 - xc: cart position
% x2 - alpha: angle of beam
% x3 - gamma: angle of bob
% p1 - xc_dot
% p2 - alpha_dot
% p3 - gamma_dot
% x = [x1 x2 x3 dx1 dx2 dx3]
syms mc msp mfp Jsp Jfp Lp Ks Lsp Lfp g ng
Kg Kt Km rmp nm Rm
syms x1 x2 x3 p1 p2 p3 Vm x4 x5 x6

%% modeling
m11=mfp+mc+msp;
m12=-msp*Lsp*cos(x2)-mfp*Lsp*cos(x2);
m13=0;
m21=-msp*Lsp*cos(x2)-mfp*Lsp*cos(x2);
m22=Jsp+mfp*(Lsp)^2+msp*(Lsp)^2;
m23=mfp*Lfp*sin(x3)*Lsp*sin(x2)+mfp*Lfp*cos(x3)*Lsp*cos(x2);
m31=-mfp*Lfp*cos(x3);
m32=mfp*Lfp*sin(x3)*Lsp*sin(x2)+mfp*Lfp*cos(x3)*Lsp*cos(x2);
m33=Jfp+mfp*(Lfp)^2;
%
n11=((ng*Kg*Kt)/(Rm*rmp))*((Kg*Km)/rmp);
n12=(msp*Lsp*sin(x2)+mfp*Lsp*sin(x2))*p2;
n13=(mfp*Lfp*sin(x3)*p3-mfp*Lfp*cos(x3));
n21=0;
n22=0;
n23=(-mfp*Lfp*sin(x3)*Lsp*cos(x2)+mfp*Lfp*cos(x3)*Lsp*sin(x3))*p3;
n31=0;
n32=(-mfp*Lfp*cos(x3)*Lsp*sin(x2)+mfp*Lfp*sin(x3)*Lsp*cos(x3))*p2;
n33=0;
%
k11=0;
k21=-msp*g*Lsp*sin(x2)-mfp*g*Lsp*sin(x2);
k31=Ks*x3-mfp*g*Lfp*sin(x3);
%
u1=((ng*Kg*Kt)/(Rm*rmp))*(nm*Vm);
%%
M= [m11 m12 m13;
    m21 m22 m23;
    m31 m32 m33];
N= [n11 n12 n13;
    n21 n22 n23;
    n31 n32 n33];
K= [k11;
    k21;
    k31];
U=[u1;0;0];

H = M*[x4;x5;x6]+N*[p1;p2;p3]+K-U;
h1=H(1);
h2=H(2);
h3=H(3);
[x4,x5,x6]=solve(h1,h2,h3,x4,x5,x6)
```

7. Conflict of Interest

All authors declare that they have no conflicts of interest.

8. Acknowledgement

This paper belongs to project T2023-55 which is funded by Ho Chi Minh city University of Technology and Education (HCMUTE). We, authors, are grateful to this support.

9. References

- [1] Faizan F., Fari F., Rehan M., Mughal S., Qadri M.T.: "Implementation of Discrete PID on Inverted Pendulum", 2010 2nd International Conference on Education Technology and Computer (ICETC), pp. 48-51, 2010, DOI: 10.1109/ICETC.2010.5529304.
- [2] Wang J.J.: "Simulation studies of inverted pendulum based on PID controllers", Simulation Modelling Practice and Theory, pp. 440-449, 2011, DOI: <https://doi.org/10.1016/j.simpat.2010.08.003>.
- [3] Chakraborty K., Mukherjee R.R., Mukherjee S.: "Tuning Of PID Controller Of Inverted Pendulum Using Genetic Algorithm", International Journal of Soft Computing and Engineering (IJSCE), Vol. 1 2, pp. 21-24, 2013, DOI: https://doi.org/10.1007/978-981-10-4762-6_38.
- [4] Razzaghi K., Jalali A.A.: "A New Approach on Stabilization Control of an Inverted Pendulum Using PID Controller", Advanced Materials Research, Vol. 403-408, pp. 4674-4680, 2012, DOI: [10.4028/www.scientific.net/AMR.403-408.4674](https://doi.org/10.4028/www.scientific.net/AMR.403-408.4674).
- [5] Sen M.A., Kalyoncu M.: "Optimisation of a PID Controller for an Inverted Pendulum Using the Bees Algorithm", Applied Mechanics and Materials, Vol. 789-790, pp. 1039-1044, 2015, DOI: [10.4028/www.scientific.net/AMM.789-790.1039](https://doi.org/10.4028/www.scientific.net/AMM.789-790.1039).
- [6] Wongsathan C., Sirima C.: "Application of GA to Design LQR Controller for an Inverted Pendulum System", International Conference on Robotics and Biomimetics, Bangkok, 2009, DOI: 10.1109/ROBIO.2009.4913127.
- [7] Banerjee R., Pal A.: "Stabilization Of Inverted Pendulum On Cart Based On Pole Placement and LQR", International Conference on Advanced Mechatronic Systems (ICAMechS), Luoyang, China, 2013, DOI: 10.1109/ICCSDET.2018.8821196.
- [8] El-Hawwary M.I., Elshafei A.L., Emar H.M., Fattah H.A.A.: "Adaptive Fuzzy Control of the Inverted Pendulum Problem", Ieee Transactions On Control Systems Technology, Vol. 14, p. 1135-1144, NO. 6, November 2006, DOI: 10.1109/TCST.2006.880217.
- [9] Meena R.I.B., Girgis E.: "Optimal fractional-order adaptive fuzzy control on inverted pendulum model", International Journal of Dynamics and Control, Vol. 9, p. 288-298, 2020, DOI: <https://doi.org/10.1007/s40435-020-00636-9>.
- [10] De Carvalho Jr. A., Justo J.F., Angélico B.A., De Oliveira A.M., Da Silva Filho D.J.I.: "Rotary Inverted Pendulum Identification for control by Paraconsistent Neural Network", IEEE Journals & Magazine, Vol. 9, p. 74155-74167, 2021, DOI: 10.1109/ACCESS.2021.3080176.
- [11] Gao H., Li X., Gao C., Wu J.: "Neural Network Supervision Control Strategy for Inverted pendulum tracking control", Discrete Dynamics in Nature and Society, Vol.2021, p. 1-14, 2021, DOI: <https://doi.org/10.1155/2021/5536573>.
- [12] Hayase T., Suematsu Y.: "Control of a flexible inverted pendulum", Advanced Robotics, vol. 8, p. 1-12, 1993.
- [13] Franco E., Astolf A., y Baen F.R.: "Robust balancing control of flexible inverted-pendulum systems", Mechanism and Machine Theory, vol. 130, pp. 539-551, 2018, DOI: <https://doi.org/10.1016/j.mechmachtheory.2018.09.001>
- [14] Jiali T., Gexu R.: "Modeling and Simulation of a Flexible Inverted Pendulum System", Tsinghua Science & Technology, Vol. 14, p. 22-26, 2009, DOI: 10.1016/S1007-0214(10)70025-0.
- [15] Apkarian H.J., Lacheray H., Martin P.: "Laboratory guide: Linear Flexible Inverted Pendulum Experiment, Markham" Ontario: MATLAB SIMULINK, 2012. Retrived from: <https://www.made-for-science.com/de/quanser/?df=made-for-science-quanser-linear-flexible-inverted-pendulum-coursewarestud-matlab.pdf>